Rectangular Patch Resonator with Laminated Ground Plane

Jean-Fu Kiang, *Member, IEEE*

Abstract— **In this paper, we analyze the effect of a laminated ground plane on the resonance frequency of rectangular patch resonators. We model each lamina of the ground plane as an anisotropic layer and use a transition matrix to relate the tangential field components in different laminae. An integral equation is formulated in the spectral domain, and Galerkin's method is applied to solve the integral equation for the resonance frequencies of the patch resonator. A perturbation approach is also derived for comparison.**

The effects of substrate dielectric are studied. The resonance frequency variation thus obtained will be useful in designing patch resonators attached to composite laminated surfaces.

I. Introduction

PATCH resonators are used as low-profile radiating elements where a rectangular patch is attached to a substrate with a ground plane [1], [2]. Conventionally, the ground plane is modeled as a perfect electric conductor. A surface impedance approach has been used to model the imperfect conductor in a layered medium [3]. In [4], the current distribution inside imperfect conductors of finite thickness is considered in analyzing the attenuation properties of microstrip lines.

In modern aircraft and vehicle designs, composite materials have been used widely in the vehicle surface to reduce the weight or the radar cross section. Take for example, a graphite-epoxy (G/E) composite is made of several laminae of epoxy rezin with conductive graphite fibers embedded in specific directions [5]. If a patch resonator is built on composite surface, details of the ground plane need to be considered.

In some circuit board fabrications, to improve the adhesion between the ground plane and substrate with temperature variation, the ground planes are made by laying one layer of metallic wires over the substrate, followed by another layer of wires perpendicular to the first layer. Thus the ground plane can be modeled as two stacking layers of anisotropic media. In each wire layer, the conductivity along the wire orientation is much higher than the perpendicular orientations. Understanding the meshed ground plane characteristics becomes practically important if we try to build a patch resonator with such a ground plane.

In this paper, we will study the effect of laminated ground planes on the resonance frequencies of a rectangular patch resonator. Each lamina of the ground plane is a periodic structure in the xy-plane. Scattering from a sandwiched layer of conducting fibers has been analyzed [6]. If the fiber spacing is comparable to wavelength, Floquet modes should be incorporated in the analysis. In [5], an anisotropic conductivity tensor is used to study the shielding effectiveness of a G/E composite. The fiber separation in each G/E lamina is a tiny fraction of a wavelength, hence using an equivalent conductivity tensor is appropriate to analyze its propagation properties.

Characteristics of a patch resonator on anisotropic substrates have been analyzed by several authors [7]–[10]. In [8], a differential matrix operator is derived from Maxwell's equations to calculate the tangential field components. This method was also used in optics [11], [12] and scattering [13]. General derivations can also be found in [14]–[17].

With either a meshed ground plane or laminated ground plane, the resonance characteristics is different from that obtained by the solid ground plane assumption. We assume that the wire/fiber spacing in each lamina of the ground plane is much smaller than a wavelength, hence each lamina can be modeled as an anisotropic layer with a conductivity tensor.

We will first formulate a transition matrix, then derive an integral equation based on the electric surface current on the rectangular patch. Galerkin's method is applied to solve for the resonance frequencies. We also derive a perturbation approach for comparison.

II. Transition Matrix

A rectangular patch resonator is shown in Fig. 1. Assume that the ground plane is composed of N laminae of homogeneous anisotropic media, and the principal axes of each lamina lie in the xy-plane. All laminae are stacked along the z-direction, and the effective permittivity ($\bar{\bar{\epsilon}}$) and conductivity ($\bar{\bar{\sigma}}$) tensors in each lamina are independent of z.

We first derive the transition matrix in the spectral domain for a single lamina. If the principal axis of $\bar{\bar{\sigma}}$ and $\bar{\bar{\epsilon}}$ skews from the x-axis by an angle α (fibers are laid from the x-axis by an angle α), $\bar{\bar{\sigma}}$ and $\bar{\bar{\epsilon}}$ can be expressed as

$$\bar{\bar{\sigma}} = \begin{bmatrix} \bar{\bar{\sigma}}_s & 0 \\ 0 & \sigma_{zz} \end{bmatrix} = \begin{bmatrix} \sigma_{xx} & \sigma_{xy} & 0 \\ \sigma_{yx} & \sigma_{yy} & 0 \\ 0 & 0 & \sigma_{zz} \end{bmatrix}$$

$$\bar{\bar{\epsilon}} = \begin{bmatrix} \bar{\bar{\epsilon}}_s & 0 \\ 0 & \epsilon_{zz} \end{bmatrix} = \begin{bmatrix} \epsilon_{xx} & \epsilon_{xy} & 0 \\ \epsilon_{yx} & \epsilon_{yy} & 0 \\ 0 & 0 & \epsilon_{zz} \end{bmatrix} \tag{1}$$

where $\bar{\bar{\sigma}}_s$ and $\bar{\bar{\epsilon}}_s$ are 2×2 tensors. $\xi_{xx} = \xi'_{xx}\cos^2\alpha + \xi'_{yy}\sin^2\alpha$, $\xi_{xy} = \xi_{yx} = (\xi'_{yy} - \xi'_{xx})\sin\alpha\cos\alpha$, $\xi_{yy} = \xi'_{xx}\sin^2\alpha + \xi'_{yy}\cos^2\alpha$, and $\xi_{zz} = \xi'_{zz}$ with ξ as either ϵ or σ. Here, ξ'_{xx}, ξ'_{yy}, and ξ'_{zz} are variables measured along the principal

Manuscript received November 7, 1994; revised June 19, 1995.

The author is with the Department of Electrical Engineering, National Chung-Hsing University, Taichung, Taiwan, ROC.

IEEE Log Number 9415633.

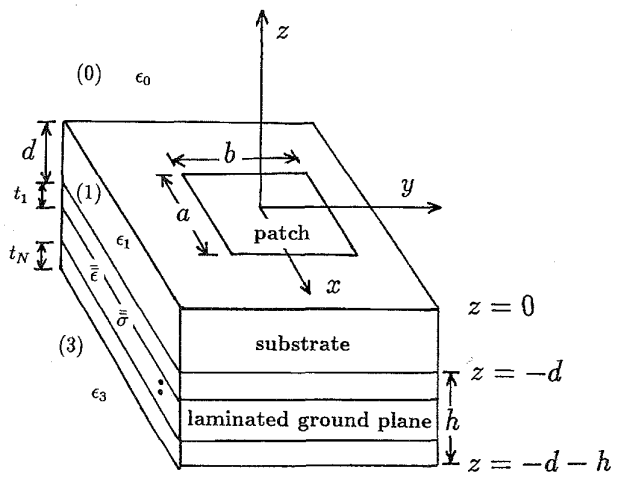

Fig. 1. A rectangular patch resonator in the presence of a laminated ground plane.

axes of the medium. We also assume an isotropic permeability of μ_o in the whole medium.

The $\overline{E}$-field, $\overline{H}$-field, and the curl operator can be decomposed into a z-component and s-(x- and y-) components first. After applying the Faraday's law and the Ampere's law to eliminate the E_z- and H_z-components, and assuming a solution with the xy-dependence of $\exp(i\overline{k}_s \cdot \overline{r}_s)$, we obtain the following state-variable equations [17]

$$\frac{d\overline{E}_s}{dz} = \overline{\overline{H}}_{12} \cdot \overline{H}_s$$
$$\frac{d\overline{H}_s}{dz} = \overline{\overline{H}}_{21} \cdot \overline{E}_s \tag{2}$$

where

$$\overline{\overline{H}}_{12} = \begin{bmatrix} \dfrac{k_x k_y}{\sigma_{zz} - i\omega\epsilon_{zz}} & i\omega\mu_o - \dfrac{k_x^2}{\sigma_{zz} - i\omega\epsilon_{zz}} \\ -i\omega\mu_o + \dfrac{k_y^2}{\sigma_{zz} - i\omega\epsilon_{zz}} & -\dfrac{k_x k_y}{\sigma_{zz} - i\omega\epsilon_{zz}} \end{bmatrix}$$
$$\overline{\overline{H}}_{21} = \begin{bmatrix} \sigma_{yx} - i\omega\epsilon_{yx} - i\dfrac{k_x k_y}{\omega\mu_o} & \sigma_{yy} - i\omega\epsilon_{yy} + i\dfrac{k_x^2}{\omega\mu_o} \\ -\sigma_{xx} + i\omega\epsilon_{xx} - i\dfrac{k_y^2}{\omega\mu_o} & -\sigma_{xy} + i\omega\epsilon_{xy} + i\dfrac{k_x k_y}{\omega\mu_o} \end{bmatrix}. \tag{3}$$

Equation (2) can be decoupled to have

$$\frac{d^2\overline{E}_s}{dz^2} = \overline{\overline{H}}_{12} \cdot \overline{\overline{H}}_{21} \cdot \overline{E}_s = \overline{\overline{H}}_e \cdot \overline{E}_s$$
$$\frac{d^2\overline{H}_s}{dz^2} = \overline{\overline{H}}_{21} \cdot \overline{\overline{H}}_{12} \cdot \overline{H}_s = \overline{\overline{H}}_h \cdot \overline{H}_s \tag{4}$$

since $\det(\overline{\overline{H}}_e) = \det(\overline{\overline{H}}_h)$ and $\mathrm{tr}(\overline{\overline{H}}_e) = \mathrm{tr}(\overline{\overline{H}}_h)$, $\overline{E}_s$ and $\overline{H}_s$ have the same eigen modes which can be expressed as $\overline{E}_s = \overline{E}_{so} e^{\gamma z}, \overline{H}_s = \overline{H}_{so} e^{\gamma z}$. The eigenvalue γ^2 can be solved from either $\det(\gamma^2\overline{\overline{I}} - \overline{\overline{H}}_e) = 0$ or $\det(\gamma^2\overline{\overline{I}} - \overline{\overline{H}}_h) = 0$. Explicitly,

$$\gamma_a^2, \gamma_b^2 = \tfrac{1}{2}\,\mathrm{tr}(\overline{\overline{H}}_e) \pm \sqrt{[\tfrac{1}{2}\,\mathrm{tr}(\overline{\overline{H}}_e)]^2 - \det(\overline{\overline{H}}_e)}.$$

The E_x- and E_y-components of the eigenvector $\overline{E}_s$ are related by $E_y = (\gamma^2 - H_{e,11})E_x / H_{e,12}$, where $H_{e,ij}$ is the ijth element of matrix $\overline{\overline{H}}_e$. The associated $\overline{H}_s$ equals to $\overline{\overline{H}}_{12}^{-1} \cdot (d\overline{E}_s/dz)$. We may express E_x as $E_x = Ae^{\gamma_a z} + Be^{-\gamma_a z} + Ce^{\gamma_b z} + De^{-\gamma_b z}$, then the associated E_y, H_x, and H_y-components become

$$E_y = \alpha_a(Ae^{\gamma_a z} + Be^{-\gamma_a z}) + \alpha_b(Ce^{\gamma_b z} + De^{-\gamma_b z})$$
$$\overline{H}_s = \overline{\overline{H}}_{12}^{-1} \cdot \begin{bmatrix} \gamma_a(Ae^{\gamma_a z} - Be^{-\gamma_a z}) + \gamma_b(Ce^{\gamma_b z} - De^{-\gamma_b z}) \\ \alpha_a\gamma_a(Ae^{\gamma_a z} - Be^{-\gamma_a z}) + \alpha_b\gamma_b(Ce^{\gamma_b z} - De^{-\gamma_b z}) \end{bmatrix} \tag{5}$$

where $\alpha_a = (\gamma_a^2 - H_{e,11})/H_{e,12}$ and $\alpha_b = (\gamma_b^2 - H_{e,11})/H_{e,12}$. Define

$$\overline{V}(\overline{k}_s, z) = [E_x(\overline{k}_s, z), E_y(\overline{k}_s, z), H_x(\overline{k}_s, z), H_y(\overline{k}_s, z)]^t$$

then we have the compact form

$$\overline{V}(\overline{k}_s, z) = \overline{\overline{P}}(\overline{k}_s, z, 0) \cdot \overline{V}(\overline{k}_s, 0)$$

with $\overline{\overline{P}}(z) = \overline{\overline{U}} \cdot \mathrm{diag}[e^{\gamma_a z}, e^{-\gamma_a z}, e^{\gamma_b z}, e^{-\gamma_b z}] \cdot \overline{\overline{U}}^{-1}$, the transition matrix between the tangential field components at $z = z$ and $z = 0$. The explicit form of $\overline{\overline{U}}$ is (6), shown at the bottom of the page, where

$$\overline{\overline{H}}_{12}^{-1} = \begin{bmatrix} h_{11} & h_{12} \\ h_{21} & h_{22} \end{bmatrix}.$$

III. Rectangular Patch Resonator

As shown in Fig. 1, the z-component of the fields in each region can be expressed as

$$E_{0z}(\overline{r}) = \iint_{-\infty}^{\infty} d\overline{k}_s e^{i\overline{k}_s \cdot \overline{r}_s} e_0(\overline{k}_s) e^{ik_{0z}z_0}$$
$$H_{0z}(\overline{r}) = \iint_{-\infty}^{\infty} d\overline{k}_s e^{i\overline{k}_s \cdot \overline{r}_s} h_0(\overline{k}_s) e^{ik_{0z}z_0}$$
$$E_{1z}(\overline{r}) = \iint_{-\infty}^{\infty} d\overline{k}_s e^{i\overline{k}_s \cdot \overline{r}_s} [e_1^U(\overline{k}_s) e^{ik_{1z}z_1} + e_1^D(\overline{k}_s) e^{-ik_{1z}z_1}]$$
$$H_{1z}(\overline{r}) = \iint_{-\infty}^{\infty} d\overline{k}_s e^{i\overline{k}_s \cdot \overline{r}_s} [h_1^U(\overline{k}_s) e^{ik_{1z}z_1} + h_1^D(\overline{k}_s) e^{-ik_{1z}z_1}]$$

$$\overline{\overline{U}} = \begin{bmatrix} 1 & 1 & 1 & 1 \\ \alpha_a & \alpha_a & \alpha_b & \alpha_b \\ \gamma_a(h_{11} + \alpha_a h_{12}) & -\gamma_a(h_{11} + \alpha_a h_{12}) & \gamma_b(h_{11} + \alpha_b h_{12}) & -\gamma_b(h_{11} + \alpha_b h_{12}) \\ \gamma_a(h_{21} + \alpha_a h_{22}) & -\gamma_a(h_{21} + \alpha_a h_{22}) & \gamma_b(h_{21} + \alpha_b h_{22}) & -\gamma_b(h_{21} + \alpha_b h_{22}) \end{bmatrix} \tag{6}$$

$$E_{3z}(\bar{r}) = \iint_{-\infty}^{\infty} d\bar{k}_s e^{i\bar{k}_s\cdot\bar{r}_s} e_3(\bar{k}_s) e^{-ik_{3z}z_3}$$

$$H_{3z}(\bar{r}) = \iint_{-\infty}^{\infty} d\bar{k}_s e^{i\bar{k}_s\cdot\bar{r}_s} h_3(\bar{k}_s) e^{-ik_{3z}z_3} \tag{7}$$

where $\bar{k}_s = \hat{x}k_x + \hat{y}k_y$, $z_0 = z + d_0, z_1 = z + d_1, z_2 = z + d_2$, and $z_3 = z + d_2$. In (7), $e_n(\bar{k}_s)(h_n(\bar{k}_s))$ is the spectral domain representation of $E_{nz}(\bar{r})(H_{nz}(\bar{r}))$ with $n = 0, 3$. In region (1), both an upward component $(e_1^U(\bar{k}_s))$ and a downward component $(e_1^D(\bar{k}_s))$ are needed to represent $E_{1z}(\bar{r})$, as is $H_{1z}(\bar{r})$. These unknowns in the spectral domain will be solved later in this section.

The tangential (to z) components of the field can be expressed as [18]

$$\bar{E}_{0s}(\bar{r}) = \iint_{-\infty}^{\infty} d\bar{k}_s e^{i\bar{k}_s\cdot\bar{r}_s} \bar{\bar{F}}(\bar{k}_s) \cdot \begin{bmatrix} -\frac{k_{0z}}{k_s} e_0(\bar{k}_s) \\ -\frac{\omega\mu_o}{k_s} h_0(\bar{k}_s) \end{bmatrix} e^{ik_{0z}z_0}$$

$$\bar{H}_{0s}(\bar{r}) = \iint_{-\infty}^{\infty} d\bar{k}_s e^{i\bar{k}_s\cdot\bar{r}_s} \bar{\bar{F}}(\bar{k}_s) \cdot \begin{bmatrix} -\frac{k_{0z}}{k_s} h_0(\bar{k}_s) \\ \frac{\omega\epsilon_0}{k_s} e_0(\bar{k}_s) \end{bmatrix} e^{ik_{0z}z_0}$$

$$\bar{E}_{1s}(\bar{r}) = \iint_{-\infty}^{\infty} d\bar{k}_s e^{i\bar{k}_s\cdot\bar{r}_s} \bar{\bar{F}}(\bar{k}_s) \cdot \begin{bmatrix} -\frac{k_{1z}}{k_s} e_1^U(\bar{k}_s) e^{ik_{1z}z_1} + \frac{k_{1z}}{k_s} e_1^D(\bar{k}_s) e^{-ik_{1z}z_1} \\ -\frac{\omega\mu_o}{k_s} h_1^U(\bar{k}_s) e^{ik_{1z}z_1} - \frac{\omega\mu_o}{k_s} h_1^D(\bar{k}_s) e^{-ik_{1z}z_1} \end{bmatrix}$$

$$\bar{H}_{1s}(\bar{r}) = \iint_{-\infty}^{\infty} d\bar{k}_s e^{i\bar{k}_s\cdot\bar{r}_s} \bar{\bar{F}}(\bar{k}_s) \cdot \begin{bmatrix} -\frac{k_{1z}}{k_s} h_1^U(\bar{k}_s) e^{ik_{1z}z_1} + \frac{k_{1z}}{k_s} h_1^D(\bar{k}_s) e^{-ik_{1z}z_1} \\ \frac{\omega\epsilon_1}{k_s} e_1^U(\bar{k}_s) e^{ik_{1z}z_1} + \frac{\omega\epsilon_1}{k_s} e_1^D(\bar{k}_s) e^{-ik_{1z}z_1} \end{bmatrix}$$

$$\bar{E}_{3s}(\bar{r}) = \iint_{-\infty}^{\infty} d\bar{k}_s e^{i\bar{k}_s\cdot\bar{r}_s} \bar{\bar{F}}(\bar{k}_s) \cdot \left[\frac{k_{3z}}{k_s} e_3(\bar{k}_s), -\frac{\omega\mu_o}{k_s} h_3(\bar{k}_s)\right]^t e^{-ik_{3z}z_3}$$

$$\bar{H}_{3s}(\bar{r}) = \iint_{-\infty}^{\infty} d\bar{k}_s e^{i\bar{k}_s\cdot\bar{r}_s} \bar{\bar{F}}(\bar{k}_s) \cdot \left[\frac{k_{3z}}{k_s} h_3(\bar{k}_s), \frac{\omega\epsilon_3}{k_s} e_3(\bar{k}_s)\right]^t e^{-ik_{3z}z_3} \tag{8}$$

where

$$\bar{\bar{F}}(\bar{k}_s) = \frac{1}{k_s}\begin{bmatrix} k_x & k_y \\ k_y & -k_x \end{bmatrix}. \tag{9}$$

At $z = 0, \bar{E}_{0s}(\bar{r}_s) = \bar{E}_{1s}(\bar{r}_s)$ implies (10) as shown at the bottom of the page.

At $z = 0, \bar{J}_s(\bar{r}_s) = \hat{n} \times [\bar{H}_{0s}(z = 0+) - \bar{H}_{1s}(z = 0-)]$ gives (11), also shown at the bottom of the page.

The tangential field components at $z = z_N = -d$ and $z = z_0 = -d - h$ are related by the transition matrix as

$$\begin{aligned} \bar{V}(\bar{r}_s, z_N) &= \begin{bmatrix} \bar{E}_{1s}(\bar{r}_s, z_N) \\ \bar{H}_{1s}(\bar{r}_s, z_N) \end{bmatrix} = \iint_{-\infty}^{\infty} d\bar{k}_s e^{i\bar{k}_s\cdot\bar{r}_s} \\ &\quad \cdot \begin{bmatrix} \bar{\bar{F}}(\bar{k}_s) \cdot \begin{bmatrix} -\frac{k_{1z}}{k_s}(e_1^U - e_1^D) \\ -\frac{\omega\mu_o}{k_s}(h_1^U + h_1^D) \end{bmatrix} \\ \bar{\bar{F}}(\bar{k}_s) \cdot \begin{bmatrix} -\frac{k_{1z}}{k_s}(h_1^U - h_1^D) \\ \frac{\omega\epsilon_1}{k_s}(e_1^U + e_1^D) \end{bmatrix} \end{bmatrix} \\ &= \iint_{-\infty}^{\infty} d\bar{k}_s e^{i\bar{k}_s\cdot\bar{r}_s} \bar{\bar{P}}(\bar{k}_s, z_N, z_0) \\ &\quad \cdot \begin{bmatrix} \bar{E}_{3s}(\bar{k}_s, z_0) \\ \bar{H}_{3s}(\bar{k}_s, z_0) \end{bmatrix}. \end{aligned} \tag{12}$$

Decomposing $\bar{\bar{P}}(\bar{k}_s, z_N, z_0)$ into four submatrices as

$$\bar{\bar{P}}(\bar{k}_s, z_N, z_0) = \begin{bmatrix} \bar{\bar{P}}_{11}(\bar{k}_s, z_N, z_0) & \bar{\bar{P}}_{12}(\bar{k}_s, z_N, z_0) \\ \bar{\bar{P}}_{21}(\bar{k}_s, z_N, z_0) & \bar{\bar{P}}_{22}(\bar{k}_s, z_N, z_0) \end{bmatrix} \tag{13}$$

then from (8) and (12), we have

$$\begin{aligned} \bar{\bar{F}}(\bar{k}_s) \cdot \begin{bmatrix} -\frac{k_{1z}}{k_s}(e_1^U - e_1^D) \\ -\frac{\omega\mu_o}{k_s}(h_1^U + h_1^D) \end{bmatrix} &= \bar{\bar{P}}_{11} \cdot \bar{\bar{F}}(\bar{k}_s) \cdot \begin{bmatrix} \frac{k_{3z}}{k_s} e_3(\bar{k}_s) \\ -\frac{\omega\mu_o}{k_s} h_3(\bar{k}_s) \end{bmatrix} \\ &\quad + \bar{\bar{P}}_{12} \cdot \bar{\bar{F}}(\bar{k}_s) \cdot \begin{bmatrix} \frac{k_{3z}}{k_s} h_3(\bar{k}_s) \\ \frac{\omega\epsilon_3}{k_s} e_3(\bar{k}_s) \end{bmatrix} \\ \bar{\bar{F}}(\bar{k}_s) \cdot \begin{bmatrix} -\frac{k_{1z}}{k_s}(h_1^U - h_1^D) \\ \frac{\omega\epsilon_1}{k_s}(e_1^U + e_1^D) \end{bmatrix} &= \bar{\bar{P}}_{21} \cdot \bar{\bar{F}}(\bar{k}_s) \cdot \begin{bmatrix} \frac{k_{3z}}{k_s} e_3(\bar{k}_s) \\ -\frac{\omega\mu_o}{k_s} h_3(\bar{k}_s) \end{bmatrix} \\ &\quad + \bar{\bar{P}}_{22} \cdot \bar{\bar{F}}(\bar{k}_s) \cdot \begin{bmatrix} \frac{k_{3z}}{k_s} h_3(\bar{k}_s) \\ \frac{\omega\epsilon_3}{k_s} e_3(\bar{k}_s) \end{bmatrix}. \end{aligned} \tag{14}$$

$$\begin{bmatrix} \frac{k_{0z}}{k_s} e_0 \\ \frac{\omega\mu_o}{k_s} h_0 \end{bmatrix} = \begin{bmatrix} \frac{k_{1z}}{k_s}\cos(k_{1z}d)(e_1^U - e_1^D) + i\frac{k_{1z}}{k_s}\sin(k_{1z}d)(e_1^U + e_1^D) \\ \frac{\omega\mu_o}{k_s}\cos(k_{1z}d)(h_1^U + h_1^D) + i\frac{\omega\mu_o}{k_s}\sin(k_{1z}d)(h_1^U - h_1^D) \end{bmatrix}. \tag{10}$$

$$\bar{J}_s(\bar{r}_s) = \iint_{-\infty}^{\infty} d\bar{k}_s e^{i\bar{k}_s\cdot\bar{r}_s} \bar{\bar{F}}(\bar{k}_s) \cdot \begin{bmatrix} \frac{\omega\epsilon_0}{k_s} e_0 - \frac{\omega\epsilon_1}{k_s}\cos(k_{1z}d)(e_1^U + e_1^D) - i\frac{\omega\epsilon_1}{k_s}\sin(k_{1z}d)(e_1^U - e_1^D) \\ \frac{k_{0z}}{k_s} h_0 - \frac{k_{1z}}{k_s}\cos(k_{1z}d)(h_1^U - h_1^D) - i\frac{k_{1z}}{k_s}\sin(k_{1z}d)(h_1^U + h_1^D) \end{bmatrix}. \tag{11}$$

Multiplying (14) by $\overline{\overline{F}}(\bar{k}_s)$ and defining $\overline{\overline{Q}}_{ij} = \overline{\overline{F}}(\bar{k}_s) \cdot \overline{\overline{P}}_{ij} \cdot \overline{\overline{F}}(\bar{k}_s)$ with $1 \le i, j \le 2$, we have

$$\begin{bmatrix} -\frac{k_{1z}}{k_s}(e_1^U - e_1^D) \\ -\frac{\omega\mu_o}{k_s}(h_1^U + h_1^D) \end{bmatrix} = \overline{\overline{Q}}_{11} \cdot \begin{bmatrix} \frac{k_{3z}}{k_s} e_3(\bar{k}_s) \\ -\frac{\omega\mu_o}{k_s} h_3(\bar{k}_s) \end{bmatrix} + \overline{\overline{Q}}_{12} \cdot \begin{bmatrix} \frac{k_{3z}}{k_s} h_3(\bar{k}_s) \\ \frac{\omega\epsilon_3}{k_s} e_3(\bar{k}_s) \end{bmatrix}$$

$$\begin{bmatrix} -\frac{k_{1z}}{k_s}(h_1^U - h_1^D) \\ \frac{\omega\epsilon_1}{k_s}(e_1^U + e_1^D) \end{bmatrix} = \overline{\overline{Q}}_{21} \cdot \begin{bmatrix} \frac{k_{3z}}{k_s} e_3(\bar{k}_s) \\ -\frac{\omega\mu_o}{k_s} h_3(\bar{k}_s) \end{bmatrix} + \overline{\overline{Q}}_{22} \cdot \begin{bmatrix} \frac{k_{3z}}{k_s} h_3(\bar{k}_s) \\ \frac{\omega\epsilon_3}{k_s} e_3(\bar{k}_s) \end{bmatrix}. \quad (15)$$

From (15), we obtain

$$\begin{bmatrix} e_1^U - e_1^D \\ h_1^U + h_1^D \end{bmatrix} = \overline{\overline{R}} \cdot \begin{bmatrix} e_3 \\ h_3 \end{bmatrix}$$

$$\begin{bmatrix} h_1^U - h_1^D \\ e_1^U + e_1^D \end{bmatrix} = \overline{\overline{S}} \cdot \begin{bmatrix} e_3 \\ h_3 \end{bmatrix} \quad (16)$$

where

$$\overline{\overline{R}} = \begin{bmatrix} -\frac{k_{3z}}{k_{1z}} Q_{11,11} - \frac{\omega\epsilon_3}{k_{1z}} Q_{12,12} & \frac{\omega\mu_o}{k_{1z}} Q_{11,12} - \frac{k_{3z}}{k_{1z}} Q_{12,11} \\ -\frac{k_{3z}}{\omega\mu_o} Q_{11,21} - \frac{\epsilon_3}{\mu_o} Q_{12,22} & Q_{11,22} - \frac{k_{3z}}{\omega\mu_o} Q_{12,21} \end{bmatrix}$$

$$\overline{\overline{S}} = \begin{bmatrix} -\frac{k_{3z}}{k_{1z}} Q_{21,11} - \frac{\omega\epsilon_3}{k_{1z}} Q_{22,12} & \frac{\omega\mu_o}{k_{1z}} Q_{21,12} - \frac{k_{3z}}{k_{1z}} Q_{22,11} \\ \frac{k_{3z}}{\omega\epsilon_1} Q_{21,21} + \frac{\epsilon_3}{\epsilon_1} Q_{22,22} & -\frac{\mu_o}{\epsilon_1} Q_{21,22} + \frac{k_{3z}}{\omega\epsilon_1} Q_{22,21} \end{bmatrix}. \quad (17)$$

Substituting (16) into (10), we obtain

$$\begin{bmatrix} e_0 \\ h_0 \end{bmatrix} = \overline{\overline{T}} \cdot \begin{bmatrix} e_3 \\ h_3 \end{bmatrix} \quad (18)$$

where

$$\overline{\overline{T}} = \cos(k_{1z}d) \begin{bmatrix} \frac{k_{1z}}{k_{0z}} & 0 \\ 0 & 1 \end{bmatrix} \cdot \overline{\overline{R}} + i \sin(k_{1z}d) \begin{bmatrix} 0 & \frac{k_{1z}}{k_{0z}} \\ 1 & 0 \end{bmatrix} \cdot \overline{\overline{S}}. \quad (19)$$

Next, substituting (16) and (18) into (11), we have

$$\overline{J}_s(\bar{r}_s) = \iint_{-\infty}^{\infty} d\bar{k}_s e^{i\bar{k}_s \cdot \bar{r}_s} \overline{J}_s(\bar{k}_s) = \iint_{-\infty}^{\infty} d\bar{k}_s e^{i\bar{k}_s \cdot \bar{r}_s} \overline{\overline{F}}(\bar{k}_s) \cdot \overline{\overline{X}} \cdot \begin{bmatrix} e_3 \\ h_3 \end{bmatrix} \quad (20)$$

where we get (21) as shown at the bottom of the page.

Thus, we have

$$\begin{bmatrix} e_3 \\ h_3 \end{bmatrix} = \overline{\overline{X}}^{-1} \cdot \overline{\overline{F}}(\bar{k}_s) \cdot \overline{J}_s(\bar{k}_s). \quad (22)$$

With (18), $\overline{E}_{0s}(\bar{r})$ can be expressed as

$$\overline{E}_{0s}(\bar{r}) = \iint_{-\infty}^{\infty} d\bar{k}_s e^{i\bar{k}_s \cdot \bar{r}_s} e^{ik_{0z}z_0} \overline{\overline{F}}(\bar{k}_s) \cdot \begin{bmatrix} -\frac{k_{0z}}{k_s} & 0 \\ 0 & -\frac{\omega\mu_o}{k_s} \end{bmatrix} \cdot \overline{\overline{T}} \cdot \overline{\overline{X}}^{-1} \cdot \overline{\overline{F}}(\bar{k}_s) \cdot \overline{J}_s(\bar{k}_s) = \iint_{-\infty}^{\infty} d\bar{k}_s e^{i\bar{k}_s \cdot \bar{r}_s} \overline{\overline{G}}(\bar{k}_s, z_0) \cdot \overline{J}_s(\bar{k}_s). \quad (23)$$

Now we impose the boundary condition that

$$\overline{J}_s(\bar{r}_s) = 0, \quad \text{outside of the strip}$$
$$\overline{E}_{0s}(\bar{r}_s) = 0, \quad \text{on the strip surface.} \quad (24)$$

Equation (24) is the dual vector integral equation to be solved for the resonance frequencies.

IV. Galerkin's Method

For a rectangular patch of width a along the x-axis and b along the y-axis, we choose a set of basis functions to represent the surface current $\overline{J}_s(\bar{r}_s)$ as

$$\overline{J}_s(\bar{r}_s) = \hat{x} \sum_{n=1}^{N_x} \sum_{m=0}^{M_x} a_{nm} f_{nm}(\bar{r}_s) + \hat{y} \sum_{n=0}^{N_y} \sum_{m=1}^{M_y} b_{nm} g_{nm}(\bar{r}_s) \quad (25)$$

where

$$f_{nm}(\bar{r}_s) = \begin{cases} \sin(n\pi x/a)\cos(m\pi y/b), \\ \qquad 0 \le x \le a, 0 \le y \le b \\ 0, \quad \text{elsewhere} \end{cases}$$

$$g_{nm}(\bar{r}_s) = \begin{cases} \cos(n\pi x/a)\sin(m\pi y/b), \\ \qquad 0 \le x \le a, 0 \le y \le b \\ 0, \quad \text{elsewhere.} \end{cases} \quad (26)$$

$$\overline{\overline{X}} = \begin{bmatrix} \frac{\omega\epsilon_0}{k_s}\frac{k_{1z}}{k_{0z}}\cos(k_{1z}d) - i\frac{\omega\epsilon_1}{k_s}\sin(k_{1z}d) & 0 \\ 0 & \frac{k_{0z}}{k_s}\cos(k_{1z}d) - i\frac{k_{1z}}{k_s}\sin(k_{1z}d) \end{bmatrix} \cdot \overline{\overline{R}} + \begin{bmatrix} 0 & i\frac{\omega\epsilon_0}{k_s}\frac{k_{1z}}{k_{0z}}\sin(k_{1z}d) - \frac{\omega\epsilon_1}{k_s}\cos(k_{1z}d) \\ i\frac{k_{0z}}{k_s}\sin(k_{1z}d) - \frac{k_{1z}}{k_s}\cos(k_{1z}d) & 0 \end{bmatrix} \cdot \overline{\overline{S}}. \quad (21)$$

Taking the Fourier transform of (25), substituting into (23), and imposing the boundary condition in (24), we have

$$\sum_{n=1}^{N_x}\sum_{m=0}^{M_x} a_{nm}\iint_{-\infty}^{\infty} d\bar{k}_s e^{i\bar{k}_s\cdot\bar{r}_s}\overline{\overline{G}}(\bar{k}_s, z_0=0)\cdot\hat{x}\tilde{f}_{nm}(\bar{k}_s) + \sum_{n=0}^{N_y}\sum_{m=1}^{M_y} b_{nm}\iint_{-\infty}^{\infty} d\bar{k}_s e^{i\bar{k}_s\cdot\bar{r}_s}\overline{\overline{G}}(\bar{k}_s, z_0=0)\cdot\hat{y}\tilde{g}_{nm}(\bar{k}_s)=0 \tag{27}$$

where

$$\tilde{f}_{nm}(\bar{k}_s)=\frac{1}{4\pi^2}\iint_{-\infty}^{\infty} d\bar{r}_s e^{-i\bar{k}_s\cdot\bar{r}_s} f_{nm}(\bar{r}_s)$$

$$\tilde{g}_{nm}(\bar{k}_s)=\frac{1}{4\pi^2}\iint_{-\infty}^{\infty} d\bar{r}_s e^{-i\bar{k}_s\cdot\bar{r}_s} g_{nm}(\bar{r}_s). \tag{28}$$

Next, we take the inner product of $\hat{x}f_{kl}(\bar{r}_s)$ and $\hat{y}g_{kl}(\bar{r}_s)$ with (27) to obtain a matrix equation as

$$\sum_{n=1}^{N_x}\sum_{m=0}^{M_x} a_{nm}\iint_{-\infty}^{\infty} d\bar{k}_s\tilde{f}_{kl}(-\bar{k}_s)\hat{x}\cdot\overline{\overline{G}}(\bar{k}_s, z_0=0)\cdot\hat{x}\tilde{f}_{nm}(\bar{k}_s) + \sum_{n=0}^{N_y}\sum_{m=1}^{M_y} b_{nm}\iint_{-\infty}^{\infty} d\bar{k}_s\tilde{f}_{kl}(-\bar{k}_s)\hat{x}\cdot\overline{\overline{G}}(\bar{k}_s, z_0=0)\cdot\hat{y}\tilde{g}_{nm}(\bar{k}_s)=0, \quad 1\le k\le N_x, 0\le l\le M_x$$

$$\sum_{n=1}^{N_x}\sum_{m=0}^{M_x} a_{nm}\iint_{-\infty}^{\infty} d\bar{k}_s\tilde{g}_{kl}(-\bar{k}_s)\hat{y}\cdot\overline{\overline{G}}(\bar{k}_s, z_0=0)\cdot\hat{x}\tilde{f}_{nm}(\bar{k}_s) + \sum_{n=0}^{N_y}\sum_{m=1}^{M_y} b_{nm}\iint_{-\infty}^{\infty} d\bar{k}_s\tilde{g}_{kl}(-\bar{k}_s)\hat{y}\cdot\overline{\overline{G}}(\bar{k}_s, z_0=0)\cdot\hat{y}\tilde{g}_{nm}(\bar{k}_s)=0, \quad 0\le k\le N_y, 1\le l\le M_y. \tag{29}$$

Equation (29) constitutes a determinantal equation to be solved for the resonance frequency.

V. Perturbation Analysis

In this section, we will derive a perturbation approach to calculate the approximate resonance frequencies. When the substrate is very thin and the composite material is very conductive, the resonance frequencies approach that of the magnetic wall cavity. In this limit, the rectangular resonator structure can be viewed as a perturbation of a rectangular resonator with a perfect conductor ground plane and perfect magnetic sidewalls. The resonance frequency shift from that of the magnetic wall cavity can be calculated as [18]

$$\Delta\omega=\omega_f-\omega_i=\frac{L}{4\langle W_T\rangle_i} \tag{30}$$

with

$$L=-i\iint_{\Delta S} dS\hat{n}\cdot(\overline{E}_i^*\times\overline{H}_f) \tag{31}$$

and

$$\langle W_T\rangle_i=\tfrac{1}{2}\epsilon_1\iiint_V dV|\overline{E}_i|^2 \tag{32}$$

where $\overline{E}_i$ and ω_i are the electric field and the resonance frequency of the unperturbed cavity, and $\overline{H}_f$ and ω_f are the magnetic field and the resonance frequency of the perturbed cavity. $\langle W_T\rangle_i$ is the unperturbed time-averaged total energy stored in the cavity, and ΔS is the surface area of the sidewalls.

In the unperturbed case, the field components are independent of z since the substrate is very thin. Thus, the only existing modes are the TM_{nm} modes of which E_z is the only nonvanishing electric field component. Explicitly,

$$\overline{E}_i=\hat{z}E_{mn}\cos(\alpha_m x)\cos(\beta_n y)$$
$$\overline{H}_i=\frac{i\omega\epsilon_1}{\alpha_m^2+\beta_n^2}E_{mn}[\hat{x}\beta_n\cos(\alpha_m x)\sin(\beta_n y) - \hat{y}\alpha_m\sin(\alpha_m x)\cos(\beta_n y)] \tag{33}$$

where $\alpha_m = m\pi/a$ and $\beta_n = n\pi/b$. The unperturbed frequency is

$$\omega_i=\frac{1}{\sqrt{\mu_o\epsilon_1}}\sqrt{\alpha_m^2+\beta_n^2}. \tag{34}$$

The induced surface current on the side of the patch attaching to the substrate is

$$\overline{J}_s(\bar{r}_s)=\begin{cases}-i\dfrac{\omega\epsilon_1 E_{mn}}{\alpha_m^2+\beta_n^2}\begin{bmatrix}\alpha_m\sin(\alpha_m x)\cos(\beta_n y)\\ \beta_n\cos(\alpha_m x)\sin(\beta_n y)\end{bmatrix}, & \bar{r}_s \text{ on the patch}\\ 0, & \bar{r}_s \text{ outside of the patch.}\end{cases} \tag{35}$$

The corresponding $\overline{H}_f$ and $\overline{J}_s(\bar{k}_s)$ are

$$\overline{H}_f=\overline{H}_{1s}=\iint_{-\infty}^{\infty} d\bar{k}_s e^{i\bar{k}_s\cdot\bar{r}_s}\overline{\overline{F}}(\bar{k}_s)\cdot\left\{\cos(k_{1z}z_1)\begin{bmatrix}-\dfrac{k_{1z}}{k_s} & 0\\ 0 & \dfrac{\omega\epsilon_1}{k_s}\end{bmatrix}\cdot\overline{\overline{S}} + i\sin(k_{1z}z_1)\begin{bmatrix}0 & -\dfrac{k_{1z}}{k_s}\\ \dfrac{\omega\epsilon_1}{k_s} & 0\end{bmatrix}\cdot\overline{\overline{R}}\right\}\cdot\overline{\overline{X}}^{-1}\cdot\overline{\overline{F}}(\bar{k}_s)\cdot\overline{J}_s(\bar{k}_s) \tag{36}$$

$$\overline{J}_s(\bar{k}_s)=\frac{\omega\epsilon_1 E_{mn}}{4\pi^2(\alpha_m^2+\beta_n^2)}\cdot\frac{[e^{-ik_x a}(-1)^m-1][e^{-ik_y b}(-1)^n-1]}{(k_x^2-\alpha_m^2)(k_y^2-\beta_n^2)}\cdot\begin{bmatrix}\alpha_m^2 k_y\\ \beta_n^2 k_x\end{bmatrix}. \tag{37}$$

Substituting (33) and (36) into (31) with $\overline{J}_s(\bar{k}_s)$ derived from (35), we have (38), as shown at the bottom of the next page, and the time-averaged stored energy is

$$\langle W_T\rangle_i=\frac{\epsilon_1}{2}|E_{mn}|^2\frac{abd}{\eta_m\eta_n} \tag{39}$$

where $\eta_m = 1$ when $m=0$, and $\eta_m = 2$ when $m>0$.

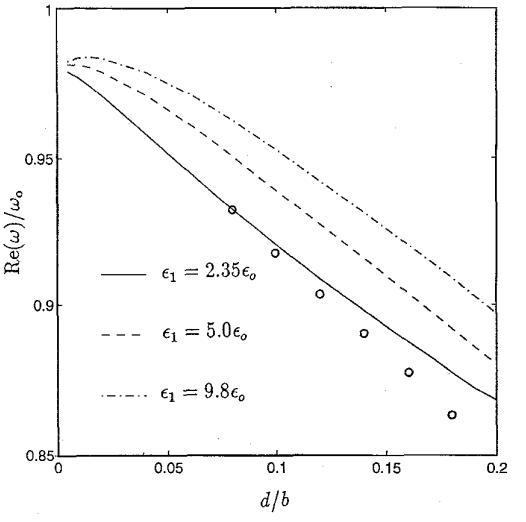

Fig. 2. Real part of (0, 1) mode resonance frequency of a rectangular patch resonator with one lamina of solid copper ground plane, $a = 18$ cm, $b = 10$ cm, $\epsilon_0 = \epsilon_3 = \epsilon_o$, $t_1 = 3$ μm, $\epsilon'_{xx} = \epsilon'_{yy} = \epsilon'_{zz} = \epsilon_o$, $\sigma'_{xx} = \sigma'_{yy} = \sigma'_{zz} = 5.8 \times 10^7$ $\mho$/m, o: results from [2].

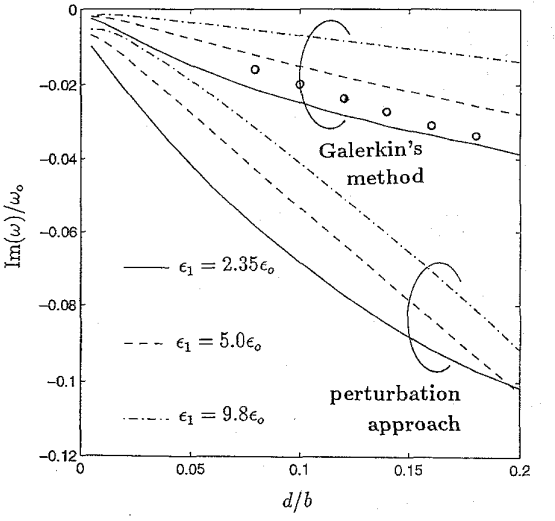

Fig. 3. Imaginary part of (0, 1) mode resonance frequency of a rectangular patch resonator with one lamina of solid copper ground plane. The parameters are the same as in Fig. 2.

VI. Results and Discussions

In Figs. 2 and 3, we show the (0, 1) mode resonance frequency of a rectangular patch resonator with a 3 μm-thick solid copper ground plane. The results with a perfect conductor ground plane and $\epsilon_1 = 2.35\epsilon_o$ from [2] are also shown for comparison. The real part does not converge to the unperturbed resonance frequency when the substrate thickness approaches zero. The imaginary part of the resonance frequency by the Galerkin's method does converge to zero at zero substrate thickness, but by the perturbation approach does not. The perturbation approach also predicts a higher imaginary frequency shift than the Galerkin's method does. Both approaches predict a slight real part decrease and imaginary part increase when d/b approaches zero for high dielectric constant $\epsilon_1 = 9.8\epsilon_o$.

Note that the (0, 1) mode is a hybrid mode corresponding to the TM_{01} mode in the perturbation analysis, but they are not exactly the same. The wave modes underneath the substrate are hybrid modes consisting of both TM and TE components. When the substrate thickness approaches zero, the TM component dominates over the TE counterpart.

We choose $N_x = M_y = 1$ and $M_x = N_y = 0$ to represent the surface current in (25). The resonance frequency thus obtained deviates from the result obtained using $N_x = M_y = 2$ and $M_x = N_y = 1$ by less than 2%.

Next, we calculate the resonance frequency of the same patch resonator in the presence of a two-lamina G/E composite ground plane. As shown in Fig. 4, the real part of the resonance frequency decreases significantly when d/b approaches zero and the higher substrate dielectric constant gives a larger extent of decrease. In Fig. 5, we show the imaginary part of resonance frequency. The results by using Galerkin's method indicate that a higher substrate dielectric constant gives a higher imaginary part at small d/b. As d gets smaller, the field beneath the patch tends to leak through the laminated ground plane. On the other hand, the perturbation approach predicts only a slight increase at small d/b for $\epsilon_1 = 9.8\epsilon_o$.

The perturbation approach works better when the perturbed field deviates slightly from the unperturbed field. The unperturbed field in (33) and the surface current in (35) are derived based on the assumption that the cavity has a perfect conductor ground plane and no field penetrates into the composite ground. With a thin substrate and low conductivity laminated composite ground, the field distribution tends to penetrate into the composite ground and deviate from the unperturbed field significantly. Hence, a large imaginary part of resonance

$$L = \frac{\omega\epsilon_1|E_{mn}|^2}{4\pi^2(\alpha_m^2+\beta_n^2)}\iint_{-\infty}^{\infty} d\bar{k}_s \cdot \frac{[e^{ik_x a}(-1)^m - 1][e^{ik_y b}(-1)^n - 1][e^{-ik_x a}(-1)^m - 1][e^{-ik_y b}(-1)^n - 1]}{(k_x^2-\alpha_m^2)(k_y^2-\beta_n^2)}$$
$$\cdot \left[-\frac{ik_x}{k_x^2-\alpha_m^2}, \frac{ik_y}{k_y^2-\beta_n^2}\right] \cdot \overline{\overline{F}}(\bar{k}_s) \cdot \left\{ \frac{\sin(k_{1z}d)}{k_{1z}} \begin{bmatrix} -\frac{k_{1z}}{k_s} & 0 \\ 0 & \frac{\omega\epsilon_1}{k_s} \end{bmatrix} \cdot \overline{\overline{S}} \right.$$
$$\left. + i\frac{(1-\cos(k_{1z}d))}{k_{1z}} \begin{bmatrix} 0 & -\frac{k_{1z}}{k_s} \\ \frac{\omega\epsilon_1}{k_s} & 0 \end{bmatrix} \cdot \overline{\overline{R}} \right\} \cdot \overline{\overline{X}}^{-1} \cdot \overline{\overline{F}}(\bar{k}_s) \cdot \begin{bmatrix} \alpha_m^2 k_y \\ \beta_n^2 k_x \end{bmatrix} \tag{38}$$

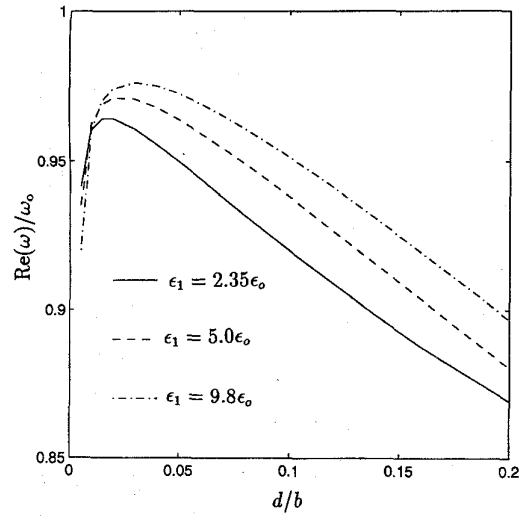

Fig. 4. Real part of (0, 1) mode resonance frequency of a rectangular patch resonator with a two-lamina G/E composite ground plane, $a = 18$ cm, $b = 10$ cm, $\epsilon_0 = \epsilon_3 = \epsilon_o$, $t_1 = t_2 = 25.4\,\mu$m, $\alpha_1 = 0$ degrees, $\alpha_2 = 90$ degrees, $\epsilon'_{xx} = \epsilon'_{yy} = \epsilon'_{zz} = 5.0\epsilon_o$, $\sigma'_{xx} = 4 \times 10^4$ $\mho$/m, $\sigma'_{yy} = \sigma'_{zz} = 50\,\mho$/m.

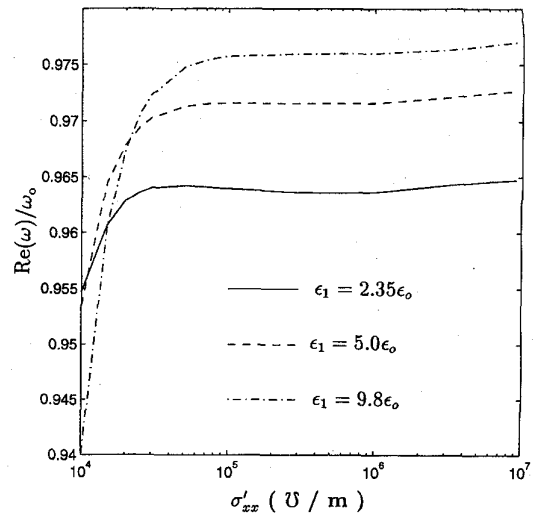

Fig. 6. Real part of (0, 1) mode resonance frequency of a rectangular patch resonator with a two-lamina G/E composite ground plane, $a = 18$ cm, $b = 10$ cm, $\epsilon_0 = \epsilon_3 = \epsilon_o$, $t_1 = t_2 = 25.4\,\mu$m, $\alpha_1 = 0$ degrees, $\alpha_2 = 90$ degrees, $\epsilon'_{xx} = \epsilon'_{yy} = \epsilon'_{zz} = 5.0\epsilon_o$, $\sigma'_{yy} = \sigma'_{zz} = 50\,\mho$/m.

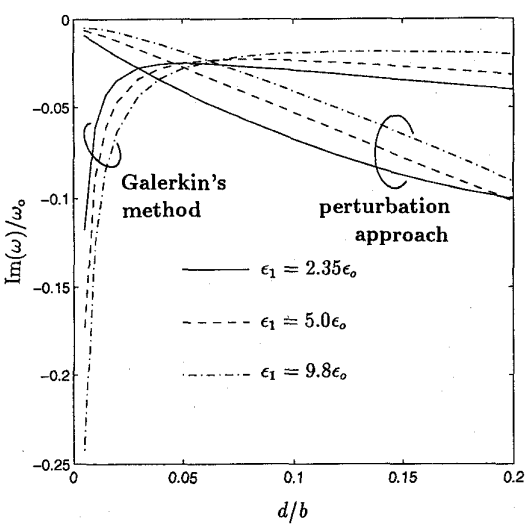

Fig. 5. Imaginary part of (0, 1) mode resonance frequency of a rectangular patch resonator with a two-lamina G/E composite ground plane. The parameters are the same as in Fig. 4.

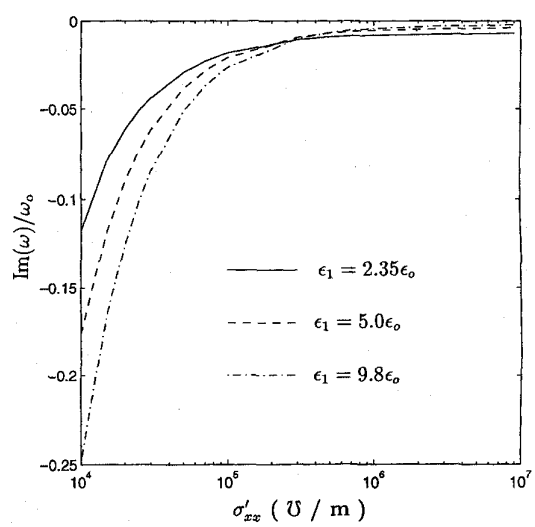

Fig. 7. Imaginary part of (0, 1) mode resonance frequency of a rectangular patch resonator with a two-lamina G/E composite ground plane. The parameters are the same as in Fig. 6.

frequency due to power leakage can not be predicted by the perturbation analysis. With high ground conductivity as in Fig. 2, the perturbed and unperturbed field distributions are similar, hence the difference between these two approaches is not as significant when the substrate thickness approaches zero. With thick substrate, the field distribution underneath the patch is hybrid, and (35) no longer adequately represents the current distribution. Hence, the results of these two approaches are different.

To check the effect of lamina conductivity on the resonance frequencies, we choose a constant value for σ'_{yy} and σ'_{zz} for the G/E composite and make σ'_{xx} a variable ranging from 10^4 to 10^7 $\mho$/m. The resonance frequency of the (0, 1) mode is shown in Figs. 6 and 7. We observe that a higher substrate dielectric constant gives a higher imaginary frequency shift at low σ'_{xx} since lower σ'_{xx} in the laminae implies that more power can penetrate through them. This observation is consistent with Figs. 4 and 5.

VII. Conclusions

We use a transition matrix to incorporate the effect of the laminated ground plane in our integral equation formulation. Galerkin's method is applied to solve for the resonance frequencies of rectangular patch resonators. The imaginary frequency shift increases when substrate thickness gets smaller and when the lamina conductivity decreases. It is caused by power leakage through the laminated ground plane. The

leakage is more significant with a higher substrate dielectric constant. The observations are useful in designing rectangular patch resonators with laminated or meshed ground planes.

ACKNOWLEDGMENT

The author would like to thank the anonymous reviewers for their precious comments.

REFERENCES

[1] W. F. Richards, Y. T. Lo, and D. D. Harrison, "An improved theory for microstrip antennas and applications," *IEEE Trans. Antennas Propagat.*, vol. AP-29, pp. 38–46, Jan. 1981.

[2] W. C. Chew and Q. Liu, "Resonance frequency of a rectangular microstrip patch," *IEEE Trans. Antennas Propagat.*, vol. AP-36, pp. 1045–1056, Aug. 1988.

[3] C. M. Krowne, "Relationships for Green's function spectral dyadics involving anisotropic imperfect conductors imbedded in layered anisotropic media," *IEEE Trans. Antennas Propagat.*, vol. 37, pp. 1207–1211, Sep. 1989.

[4] J.-F. Kiang, "Integral equation solution to the skin effect problem in conductor strips of finite thickness," *IEEE Trans. Microwave Theory Tech.*, vol. 39, pp. 452–460, Mar. 1991.

[5] M.-S. Lin and C. H. Chen, "Plane-wave shielding characteristics of anisotropic laminated composites," *IEEE Trans. Electromagn. Compat.*, vol. 35, pp. 21–27, Feb. 1993.

[6] L. N. Medgyesi-Mitschang, and J. M. Putnam, "Scattering from composite laminate strips," *IEEE Trans. Antennas Propagat.*, vol. 37, pp. 1427–1436, Nov. 1989.

[7] K.-L. Wong, J.-S. Row, C.-W. Kuo, and K.-C. Huang, "Resonance of a rectangular microstrip patch on a uniaxial substrate," *IEEE Trans. Microwave Theory Tech.*, vol. 41, pp. 698–701, Apr. 1993.

[8] T. Q. Ho, B. Beker, Y. C. Shih, and Y. Chen, "Microstrip resonators on anisotropic substrates," *IEEE Trans. Microwave Theory Tech.*, vol. 40, pp. 762–765, Apr. 1992.

[9] R. M. Nelson, D. A. Rogers, and A. G. D'assuncao, "Resonant frequency of a rectangular microstrip patch on several uniaxial substrates," *IEEE Trans. Antennas Propagat.*, vol. 38, pp. 973–981, July 1990.

[10] D. M. Pozar, "Radiation and scattering from a microstrip patch on a uniaxial substrate," *IEEE Trans. Antennas Propagat.*, vol. AP-35, pp. 613–621, June 1987.

[11] D. W. Berreman, "Optics in stratified and anisotropic media: 4 × 4-matrix formulation," *J. Opt. Soc. Am.*, vol. 62, pp. 502–510, Apr. 1972.

[12] O. Schwelb, "Stratified lossy anisotropic media: General characteristics," *J. Opt. Soc. Am. A*, vol. 3, pp. 188–193, Feb. 1986.

[13] M. A. Morgan, D. L. Fisher, and E. A. Milne, "Electromagnetic scattering by stratified inhomogeneous anisotropic media," *IEEE Trans. Antennas Propagat.*, vol. AP-35, pp. 191–197, Feb. 1987.

[14] F. L. Mesa, R. Marques, and M. Horno, "A general algorithm for computing the bidimensional spectral Green's dyad in multilayered complex bianisotropic media: The equivalent boundary method," *IEEE Trans. Microwave Theory Tech.*, vol. 39, pp. 1640–1649, Sep. 1991.

[15] J. L. Tsalamengas and N. K. Uzunoglu, "Radiation from a dipole in the proximity of a general anisotropic grounded layer," *IEEE Trans. Antennas Propagat.*, vol. AP-33, pp. 165–172, Feb. 1985.

[16] C. M. Krowne, "Determination of the Green's function in the spectral domain using a matrix method: Application to radiators or resonators immersed in a complex anisotropic layered medium," *IEEE Trans. Antennas Propagat.*, vol. AP-34, pp. 247–253, February 1986.

[17] W. C. Chew, *Waves and Fields in Inhomogeneous Media*. New York: Van Nostrand Reinhold, 1990.

[18] J. A. Kong, *Electromagnetic Wave Theory*, 2nd ed. New York: Wiley, 1990.

Jean-Fu Kiang (S'88–M'89) was born in Taipei, Taiwan, ROC on February 2, 1957. He received the B.S.E.E. and M.S.E.E. degrees from National Taiwan University, and Ph.D. degree from MIT in 1979, 1981, and 1989, respectively.

He has been with the IBM Watson Research Center, Bellcore, and Siemens. He is now with the Department of Electrical Engineering, National Chung Hsing University, Taichung, Taiwan.